Carbon and Metal Doped Polyaniline (PANI) for Energy Storage

Abdallah Ramadan and Wegdan Ramadan

Abstract With the depletion of traditional fossil fuels, rising pollution levels and fast growth of the global economy. New technology for energy conversion and storage, as well as efficient, sustainable energy sources, are all urgently needed. The development of supercapacitors (SCs) as an energy storage device has received a lot of interest in recent years. SCs are comparable to dielectric capacitors in terms of their high-power density, cyclic stability, and discharge rate. In addition, a high energy density that is comparable to batteries. In this chapter, polyaniline (PANI) based materials for electrochemical supercapacitor (ESs) electrodes are thoroughly reviewed. Pure PANI electrodes have low cycle life, low power density, and poor mechanical stability resulting from the swelling and shrinkage during the charging and discharging processes. Nevertheless, the development of nanocomposite of PANI with carbon materials or metal compounds could overcome the drawbacks of pure PANI and achieve higher electrochemical performance. Capacitance, energy, power, cycle performance, and rate capability have all been used to evaluate the performance of nanocomposites.

Graphical Abstract See Scheme 1.

Keywords Energy storage · Supercapacitors · PANI · Electrochemical double-layer capacitors · Pseudocapacitors

1 Introduction

Due to the depletion and shortage of non-renewable fossil fuels-based energy sources, a serious challenge in the current century is the energy crisis [26]. Additionally, the environment, people, and human activities are negatively impacted by the growing emissions of pollutants from nonrenewable energy (oil, gas, and coal). According to the Environmental Protection Agency (EPA), Carbon dioxide (CO_2) makes up 82%

A. Ramadan · W. Ramadan (✉)
Physics Department, Faculty of Science, Alexandria University, Alexandria 21511, Egypt
e-mail: wegdan.ramadan@alexu.edu.eg

I. Uddin and I. Ahmad (eds.), *Synthesis and Applications of Nanomaterials and Nanocomposites*, Composites Science and Technology,
https://doi.org/10.1007/978-981-99-1350-3_12

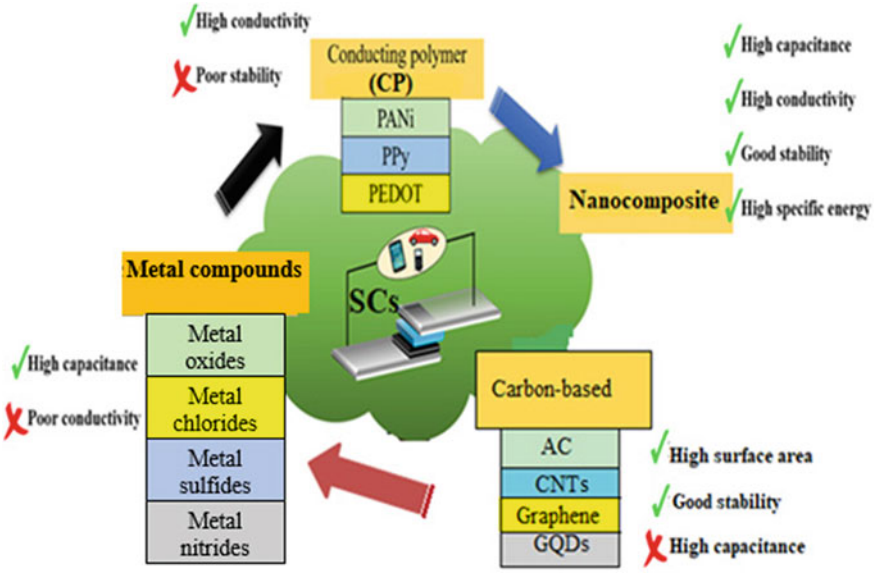

Scheme 1 Electrode materials of supercapacitor with advantages and disadvantages [35]

of emissions that are classified as greenhouse gases, followed by methane (CH_4), 9%, nitrates (NOx), 6%, and fluorinated gases (perfluorocarbons, hydrofluorocarbons, and sulfur hexafluoride), which make up 3%. Climate change consequences have been made worse by greenhouse gas emissions. These outcomes have pushed research efforts towards the creation of renewable energy sources. Energy storage devices are necessary when harvesting energy from renewable sources like photovoltaic panels or wind farms because the captured energy (such as wind or solar energy) is not always available. For example, the sun doesn't shine every day and night, and the wind doesn't always blow when we need it to. Consequently, one of the key problems that will improve the use of sustainable energies in the future is energy storage, particularly electrical energy storage. Among various energy storage technologies, lithium-ion batteries (LIBs) and supercapacitors hold great promise in broad applications such as portable electronics, smart grids and electrical vehicles [6]. Since the Sony Company first began selling LIBs in 1991, this type of secondary battery has become increasingly common in people's daily lives. Because LIBs have a high energy density of 150–200 Wh/kg, they may store electrical energy in portable devices. With a power density at least two orders of magnitude lower than that of fossil fuels, LIBs are very difficult to compare with them. Because of this, a significant number of LIBs are required to replace fuels, which sharply increases the mass of products. Different electrical energy storage devices and conversion technologies (Fig. 1) can be identified by many parameters, including energy storage mechanisms, charging and discharging processes, energy, and power densities, which define their

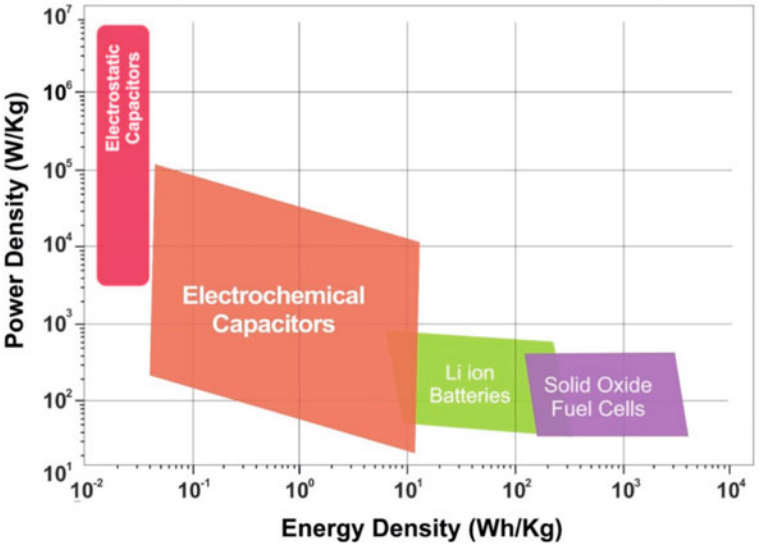

Fig. 1 Ragone plot for various electrical energy storage devices (figure used by permission of AIP Publishing) [1]

uses. Because of their slow discharge process, batteries may be employed for long-term and steady energy storage density. On the other hand, Capacitors can be used in applications that demand quick energy transmission due to their fast charging and discharging capabilities. Between traditional capacitors and batteries, supercapacitors, also known as ultracapacitors or electrochemical capacitors ESs, are a new energy storage technology. Due to its many advantages over lithium-ion batteries, such as quick charging and discharging, enormous power density, wide working temperature ranges, and extended service life cycles, supercapacitors have gained increased attention in recent years. As a result, ESs have been found to be readily applicable in a wide variety of important applications such as hybrid and electrical vehicles, portable electronics, backup power supplies, aircraft, and smart grids [9]. Batteries, capacitors, and supercapacitors are compared in Table 1 in terms of their characteristics and performance.

2 Fundamentals of Supercapacitors

A basic supercapacitor consists of two plates (current collector) coated with porous materials and separated by a porous separator soaked in an electrolyte. Each component plays an important part in determining a supercapacitor's overall performance. The supercapacitor electrode materials are deposited on conductive substrates called current collectors, it allows electrons to travel in the direction of the electrode's

Table 1 Comparison of conventional capacitor, supercapacitor and battery (table used by permission of Elsevier) [63]

Parameters	Conventional capacitor	Supercapacitor	Battery
Time of charge	10^{-6}–10^{-3} s	Sec to min	0.03–3 h
Time of discharge	10^{-6}–10^{-3} s	Sec to min	1–5 h
Energy density (Wh/kg)	<0.1	Up to 1091	Up to 1,606
Power density (W/kg)	>10,000	Up to 196,000	<1000
Cycle life	>500,000	>100,000	500–2000
Charge/discharge efficiency	~1.0	0.9–0.99	0.7–0.85

thickness instead of along the electrode's length vastly reducing the charge transport distance [86]. The porous separator allows charge transfer, and the electrolyte interacts with both electrodes. Because they determine the performance of supercapacitors, particularly the energy/power densities and life cycles of a supercapacitor, electrolytes (salt and solvent) used in supercapacitor cells are as important as the electrode materials. The electrolytes also influence the series resistance and the operating voltage of the cell. Finally, the electrode material is the most important component to achieve significant improvements in supercapacitor performance. Below is a list of the characteristics an electrode material must possess.

- To create electrochemical double-layer capacitors, a high specific surface area is required, generally between 1000 and 2000 m^2g^{-1}.
- Controlled distribution of pore size.
- Reversible redox reactions to prevent stability loss.
- Electrochemical stability beyond the limit of electrolyte decomposition.
- Surface wettability of the electrolyte.

3 Types of Supercapacitors

Based on the mechanism of charge and discharge process, there are two main types of supercapacitors as shown in Fig. 2 namely: non-Faradic, electrochemical double-layer capacitors (EDLCs) and pseudocapacitors (or redox-based electrochemical capacitors, Faradic). However, there is a hybrid type that combines the mechanism of both types mentioned above, hybrid electrochemical capacitors.

3.1 Electrochemical Double Layer Capacitors

The EDLC supercapacitor type is the first family of supercapacitors that employ porous carbon-based materials with a large specific surface area as the electrode

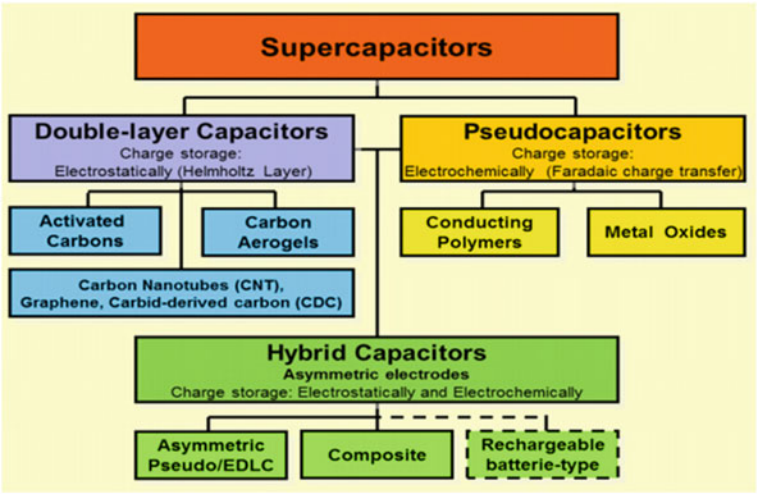

Fig. 2 Different types of supercapacitor electrodes (figure used by permission of Elsevier) [23]

material. To be more specific, the charging-discharging of an EDLC is by the accumulating of electrolyte ions onto the surface of a porous electrode by polarization. The solvated ions flow towards the two carbon electrodes when DC voltage is applied, passing across the separator to create an electric double-layer that stores the electric charges as seen in Fig. 3. The two parallel charge layers that surround the plate are referred to as the double layer.

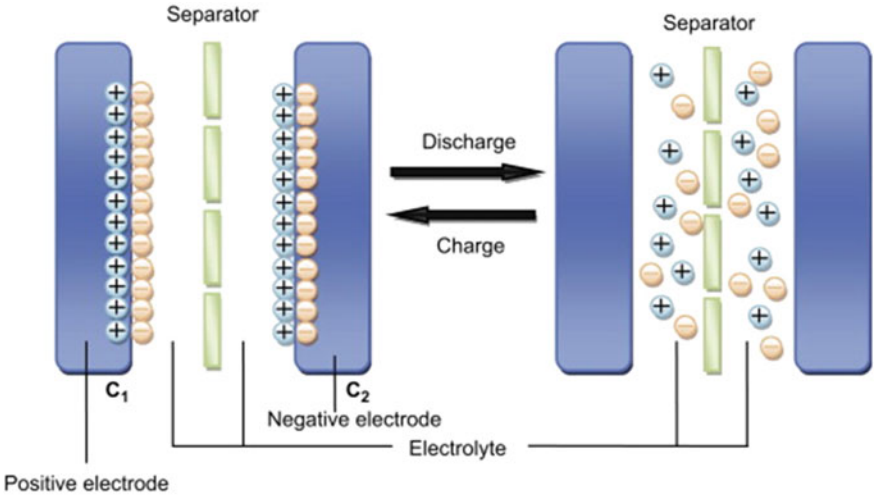

Fig. 3 Charged and discharged mechanism of an electric double layer capacitor (figure used by permission of Elsevier) [41]

The principle of EDLCs is like that in conventional capacitor, however EDLCs show high capacitance due to their maximum effective surface area and very small charge separation distances [63]. EDLCs exhibit excellent cycling stability due to the absence of chemical or composition changes associated with non-faradaic process and electrostatic charge transfer in this device is completely reversible. In EDLCs, the capacitance is related to the accumulation and separation of net electrostatic charge at the electrolyte– electrode interface. In this case, the net negative charges (mainly electrons) are accumulated at the surface of the electrode, while positive charges with an equal number (mainly cations) are accumulated near surface of the electrode facing the electrolyte solution, forming electric double-layers. Therefore, the level of the capacitance is thus determined by surface characteristics of the electrode materials. However, there is always a limitation in the magnitude of capacitance.

3.2 Electrochemical Pseudocapacitors

Unlike EDLCs, some electrochemically active materials called pseudocapacitive materials could present much higher capacitance. Pseudocapacitive materials are the second type of materials used in supercapacitors where the charging-discharging of pseudocapacitors happens at the electrode surface or close to it through fast and reversible redox reactions between electrolyte ions and electroactive species [34]. The common materials that exhibit pseudocapacitive behavior are conducting polymers and transition metal oxides/hydroxides [77]. The redox process can be described as:

$$O_X + ne^- \iff R_d \tag{1}$$

where O_X and R_d are the oxidant and the reductant which are insoluble in the electrolyte solution, n is the number of transferred electrons (e^-) in the redox reaction. Due to the redox reactions, the change in quantity of the produced charge (Δq) is a continuous function of the change in applied potential (ΔV), while the ratio $\Delta q/\Delta V$ is defined as the pseudocapacitance. On the one hand, pseudocapacitance materials such as conducting polymers and metal oxides can remarkably enhance the capacitance and energy stored of supercapacitors. On the other hand, because to the inadequate reversibility of the redox reaction, which affects the shape of the electrode, it displays limited mechanical stability and a short cycle life [61]. The comparison between two types of supercapacitors are summarized in Table 2.

3.3 Hybrid Electrochemical Capacitors

The hybrid type supercapacitors are an energy storage device which exploits the advantages of EDLC and the pseudocapacitors using composites or two asymmetric electrodes. The high power density of the EDLC and higher capacitance and energy

Table 2 Comparison between electrical double layer capacitor and pseudocapacitor

	Electric double layer capacitor	Pseudocapacitor
Storage mechanism	Electrostatic adsorption (non-faradaic process)	Redox reactions on electrodes (faradaic process)
Capacitance	Capacitance remains constant	Capacitance changes with voltage
Energy density	Low	High
Power	High power due to good diffusion	Low Power due to kinetic limitations
Diffusion resistance	Low	High
Reversibility	High reversibility	Moderate reversibility
Cycle life	Good cyclability	Moderate cyclability
Potential window	Narrow (1–3 V)	Large (1–5 V)

density of the pseudocapacitors is combined to form a device with better performance [47]. A single electrode in a hybrid configuration system that combines carbon-based materials with conducting polymers or metal oxides provides the advantages of both physical and chemical charge storage mechanisms. Asymmetric supercapacitor denotes to the combination of two separate electrode materials that use two distinct storage mechanisms. Ideally, a pseudocapacitive material electrode provides high energy density while the EDLC material electrode furnishes the system with high power capability [71].

4 Electrochemical Evaluation

The electrochemical assessment is based on their specific capacitance and capacity, as well as their energy and power densities. Different approaches, including as cyclic voltammetry (CV), and galvanometric charge discharge technique (GCD) can be used to calculate the above-mentioned parameters. These parameters are measured using techniques such as three electrode and two electrode configurations.

Because it is simple to determine the cycle life, CV has emerged as a key technique for assessing the performance of SCs. Additionally, the information on the impacts of internal resistance and the ensuing dissipative losses may be discovered by analyzing the shapes of the voltammograms as a function of scan rate s. The form of the cyclic voltammogram for EDLCs should resemble a rectangle, confirming no chemical reaction as in Fig. 4a, the rectangular shape is distorted with reversible oxidation and reduction peaks for the pseudocapacitive material, indicating a Faradaic redox process, as shown in Fig. 4b. CV data can be utilized to determine the specific capacitance Cs of an electrode material by calculating the area enclosed in cyclic voltammogram $\int \boldsymbol{I}(\boldsymbol{V}) * \boldsymbol{dV}$ using the following formula [60]:

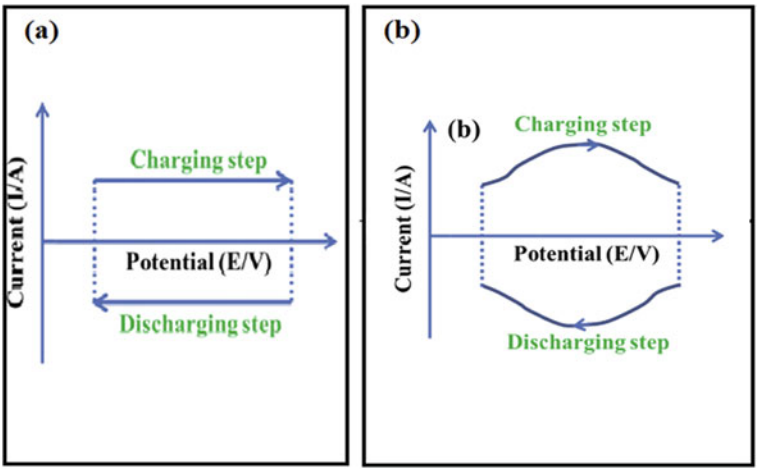

Fig. 4 Cyclic voltammograms of **a** EDL capacitor and **b** pseudo-capacitor (figure used by permission of Elsevier) [66]

$$Cs = \frac{\int I(V) * dV}{2m * s * \Delta V} \tag{2}$$

where **m** (g) is the mass loading of active material, ΔV (V) is the potential window, and **s** (mV/s) is the scan rate

The galvanostatic charge and discharge method is a more precise approach than the CV method for determining the specific capacitance of active materials. The working electrode is exposed to positive and negative continuous currents that charge and discharge the electrode within a predetermined voltage range while timing the process. Figure 5 displays a typical GCD curve that plots the voltage as a function of time. The specific capacitance Cs by F/g related to the discharge current density (I) by A/g through the relation [61, 73].

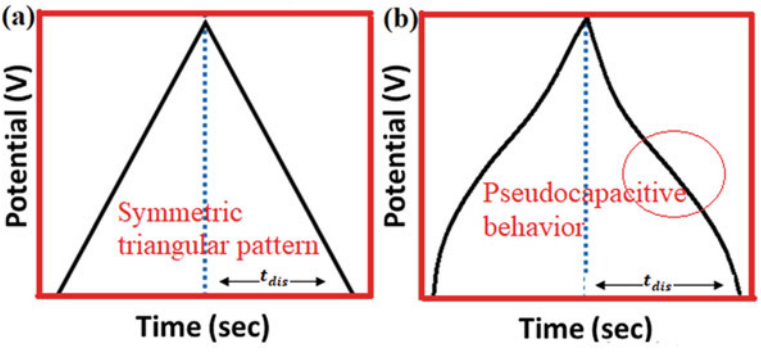

Fig. 5 GCD curves of **a** EDL capacitor and **b** pseudo-capacitor

$$Cs = \frac{I * t_{dis}}{m * \Delta V} \tag{3}$$

where t_{dis} **(s)** is the time of discharge and ΔV (V) is the working potential.

The characteristics of the active material are determined by the type of the GCD profiles, much like with the CV curves. Due to their consistent charge distributions during the charge–discharge process, an ideal EDLC profile has a linear GCD (Fig. 5a). The oxidation and reduction processes that occur throughout the charge–discharge process cause the pseudo-/Faradaic supercapacitors to have a non-linear GCD profile (Fig. 5b). To learn more about a supercapacitor electrode's electrochemical performance, the GCD measurement is required. It is used to do additional calculations about electrochemical characteristics including energy, power densities, and capacitance retention. The energy density (E) and power density (P) can be calculated using the following equations [91]:

$$E(Wh/Kg) = \frac{1}{2} * Cs * V^2 * \frac{1000}{3600} \tag{4}$$

$$P(W/Kg) = \frac{E}{t_{dis}} * 3600 \tag{5}$$

where Cs (F/g) is the specific capacitance, V (V) is the potential window and t_{dis} **(s)** is the discharge time corresponding to Cs calculated from GCD curve.

5 Polyaniline PANI

The most studied conducting polymer among the family of conducing polymers is polyaniline (PANI) due to its interesting characteristics such as ease of synthesis, doping, dedoping, low cost, mechanical flexibility, chemical properties, and environmental compatibility. There are numerous ways to synthesize polyaniline, including chemical and electrochemical polymerization. Using chemical polymerization as an example, aniline monomer is placed in an aqueous acid solution and chemical oxidants such as ammonium persulfate or ferric chloride. The polyaniline precipitates out of the chemical reaction solution. When preparing PANI nanocomposites, chemical synthesis of polyaniline provides much greater flexibility for managing the nucleation and growth mechanisms throughout the polymerization process [14]. While electrochemical polymerization is typically performed in a three-electrode electrochemical cell with an electrolyte that supports the electrochemical reaction and dissolves the aniline monomer. The monomers oxidized by repeating cycles between a potential window where the oxidation takes place and the polymer will then be electrodeposited directly onto the substrate which is a worthwhile advantage for the fabrication of binder-free supercapacitors [53].

5.1 PANI-Based Materials for Pseudocapacitors

Morphology is one of the primary factors affecting PANI's supercapacitive behavior. Varying the PANI morphology during the preparation can lead to better performance of supercapacitor [14]. Guan and coworkers [21] reported that adding a small amount of para-phenylenediamine (PPD) as additive during the polymerization of aniline can lead to the formation of longer, less entangled PANI nanofibers, which significantly enhances the electrochemical performance of PANI. Even in two electrode cells where the electroactive material is not immersed in the electrolyte to expand the electrode/electrolyte contact, the function of PANI morphology is crucially important. Also, changing the chemical polymerization temperature can produce different morphologies of PANI which could provide different cyclability. Porous PANI can also considerably enhance the performance of supercapacitor due to increasing the electrochemically accessible surface area. Sharma and coworkers [64] synthesized a nanoporous hypercrosslinked PANI with a S_{BET} of 1059 m^2/g which could deliver a specific capacitance of 410 F/g with outstanding cycling stability with 100% of the capacity retention after 1000 cycles. The electrochemical performance based on different morphologies of PANI reported in the literature are listed in Table 3.

The type of the dopant ions, electrolyte, pH of the solution, the substrate, and the deposition conditions all have an impact on the electrochemical and mechanical characteristics of the PANI supercapacitor electrode, which in turn has an impact on the capacitance of the PANI electrode [18]. The main drawbacks of PANI are the poor mechanical stability and solubility. As a result of repeated redox reactions, PANI suffer several physical/chemical changes, including swelling, shrinking, cracking or breaking, which over time reduces the material's performance. Therefore, the synthesis of composite materials may be a promising choice to improve the mechanical performance of PANI.

6 PANI/Carbon Based Material Composites

The aim of developing composite material electrodes is to incorporate the desirable characteristics of the various materials into a single electrode in order to improve stability and capacitance. Additionally, asymmetric type supercapacitors employ nanocomposite electrodes to boost operating voltage to enhance energy density. The electrodes in the PANI-carbon composites have not only efficient pseudocapacitive reactions due to synergistic effects, but also better rate capability due to the substrate's high conductivity and super cycle stability due to the excellent mechanical properties of the supporting carbon materials. Due to synergistic effects, the electrodes in PANI-carbon composites not only have effective pseudocapacitive reactions but also better rate capability and super cycle stability due to the substrate's high conductivity and the superior mechanical properties of the supporting carbon materials, respectively [45].

Table 3 Capacitance performance of different morphologies of PANI

PANI morphology	Electrolyte	Current collector	Specific capacitance	Capacitance retention	Refs.
Nanoporous PANI	1 M H_2SO_4	Carbon paper	350 F/g at 1 A/g	99% after 500 cycles at 40 A/g	[17]
PANI nanowires	1 M H_2SO_4	Stainless steel	742 F/g at 23 A/g	92% after 1500 at 3 mA/cm^2	[22]
PANI Nanofibers	1 M H_2SO_4	Stainless steel mesh	548 F/g at 0.18 A/g	75% after 1000 cycles at 1 A/g	[21]
Nanofibrous PANI	1 M H_2SO_4	Stainless steel	839 F/g at 10 mV/s	90.71% after 1000 cycles at 20 mV/s	[10]
Nanofibrous PANI	1 M H_2SO_4	Stainless steel	861 F/g at 10 mV/s	82% after 2000 cycles at 100 mV/s	[11]
Nanowire arrays	1 M $HClO_4$	Au plate	950 F/g at 1 A/g	88% after 500 cycles at 20 A/g	[72]
PANI nanowhiskers	1 M H_2SO_4	Wafer	470 F/g at 1 A/g	90.4% after 1000 cycles at 1 A/g	[81]
PANI nanobelts	1 M H_2SO_4	Ti sheet	873 F/g at 10 mV/s	96.5% after 1000 cycles at 10 mV/s	[37]
PANI nanotubes	1 M H_2SO_4	Glassy carbon	714 F/g at 0.5 mA	85% after 500 cycles at 1 mA	[65]
PANI nanospheres	1 M H_2SO_4	Graphitized carbon paper	345 F/g at 1 A/g	58% after 5000 cycles at 10 A/g	[8]
PANI nanosheets	1 M H_2SO_4	Glassy carbon	272 F/g at 1 A/g	50% after 1500 cycles at 3 A/g	[49]
PANI nanolayers	1 M H_2SO_4	ITO nanowires	738 F/g at 4 A/g	100% after 700 cycles at 4 A/g	[67]
PANI nanogranules	0.1 M H_2SO_4	Carbon paper	500 F/g at 1.5 A/g	80% after 5000 cycles at 1.5 A/g	[40]
PANI nanorods	1 M H_2SO_4	–	297 F/g at 1 A/g	65% after 1300 cycles at 100 mV/s	[74]
PANI nanofibers	1 M H_2SO_4	Stainless steel mesh	252 F/g at 0.5 A/g	76% after 1000 cycles at 2 A/g	[27]

6.1 PANI/Activated Carbon

Activated carbons ACs are one of the cheapest materials which generated by either physical or chemical activations of natural precursors (e.g. wood, coal, nutshell, etc.) [89] The specific capacitance values of supercapacitor electrode based on activated

carbon are typically between 100 and 300 F/g in both aqueous and organic electrolyte operating in potential windows between 1 and 3 V. The main drawback of ACs for supercapacitor application is the wide distribution of pore size, including micropores (<2 nm), mesopores (2–50 nm) and macropores (>50 nm) [56]. Since not all these pores are efficient for supercapacitor energy storage, Micropores with a diameter around 1 nm are not accessible to most of the organic electrolyte ions. These unnecessary micropores not only increase the volume that not contributing to the charge storage, but also hinder the electrical conductivity, limit their energy density (5–8 Wh/kg) and power density [88]. To solve this issue, nanocomposite of PANI and ACs have been investigated to enhance electrochemical performance. PANI nanorods uniformly polymerized onto the cellulous-derived highly porous activated carbons (C-ACs) framework by a chemical polymerization process have been investigated as a supercapacitor electrode material by Zhang and coworkers [93]. Due to their great electron conductivity, rapid ion transit, quick and stable surface redox reactions, PANI/C-AC composites with a 3D and hierarchically porous structure were able to achieve good capacitive performance. The PANI/C-AC composites displayed a specific capacitance of 765 F/g at a current density of 1 A/g, a specific power of 14 kW/kg, and a specific energy of 22.3 Wh/kg at a scan rate of 10 mV/s. Additionally, PANI/C-ACs composites shown outstanding cycling stability with 91% capacitance retention after 5000 cycles in a symmetric two-electrode system, in contrast to PANI electrodes, which display 82% capacitance retention. Furthermore, PANI/C-ACs have a higher rate capability because the 3D C-ACs skeletons provide enough mechanical support to avoid PANI volumetric changes during the charge/discharge process. As a result, PANI/C-ACs are potential electrode materials for high-performance SCs.

To overcome the low conductivity and hydrophobicity of ACs, nitrogen doped ACs been investigated for the purpose of increasing specific capacitance. The purpose of nitrogen doping is to increase pseudo-capacitance as a result of the redox reaction that occurs in the nitrogen-contained functional groups. Furthermore, the functional groups improve the electrode's wettability, resulting in an increase in capacity.

Yu and coworkers [88] developed hierarchical nitrogen-doped porous carbon (HPC)/polyaniline (PANI) using wheat flour as carbon precursor, as shown in Fig. 6. The PANI nanowire arrays were well-ordered on both the interior and external surfaces of the hierarchical porous HPC, facilitates the electrolyte ion into the whole electrode and ensures the highly efficient charge storage, resulting in a high specific capacitance of 1080 F/g. The 3D interconnected honey-comb-like porous structure with nitrogen doping can further increase the electrode's surface wettability and provide mechanical support for PANI nanowires.

6.2 PANI/Carbon Nanotubes

Carbon nanotubes (CNTs) have gained popularity as promising materials in an energy storage device as a result of their unique properties. These properties such as large

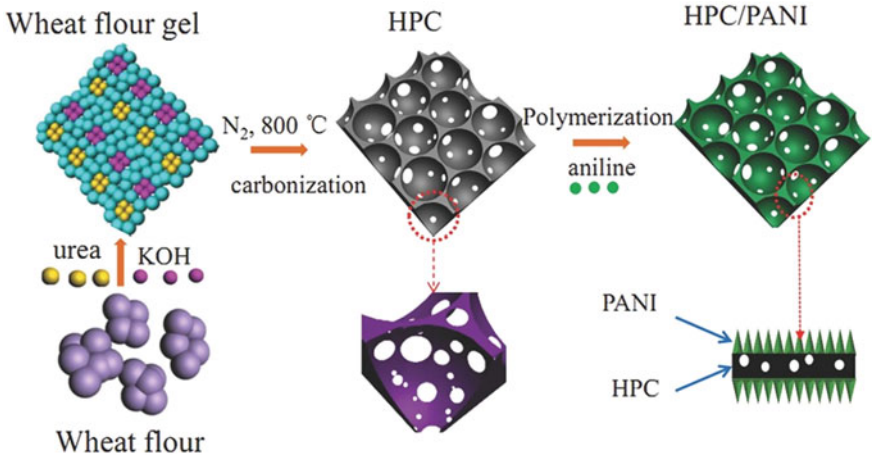

Fig. 6 Schematic illustration for the preparation of hierarchical nitrogen-doped porous carbon HPC/PANI composites (figure used by permission of John Wiley and Sons) [88]

surface area ($S_{BET} = 1600\ m^2\ g^{-1}$), different spaces for storage the electrolyte ions based on their structure, light weight, high electrical conductivity (=105 S cm^{-1}) and mechanical properties [63]. SWCNT, MWCNT, and functionalized CNT are examples of CNT layers that may be used to achieve different characteristics in supercapacitors. Surface functionalization of hydrophilic groups increased the wettability of CNTs in solvents [75]. In recent years, PANI/CNT composites have received a lot of interest in the field of energy storage based on the PANI or CNTs alone. CNT facilities the electrolyte ions to diffuse into the PANI/CNT nanocomposite electrode materials and can also improve the cycle stability of the composite during charging/discharging. Furthermore, the greater mechanical strength of PANI/CNTs electrodes allows us to construct lightweight, flexible, and foldable supercapacitors with thinner separators, eliminating the need for a binder or heavy metal foil current collectors [45]. To enhance capacitive performance, smaller size of CNT arrays with hierarchically porous structures should be aligned, for example, Zhang and coworkers [90] prepared core–shell structured PANI/CNTs arrays composite Using an electrodeposition approach. PANI/CNTs electrode material showed specific capacitances as high as 1030 F/g, excellent rate capability (95% capacity retention at 118 A/g) and great stability (5.5% capacity loss after 5000 cycles).

A plasma polymerization method was developed by Hussain and coworkers [29] to synthesize a PANI/CNT composite that is green, simple, fast, oxidizers and binder free. It produces a pinhole-free ultra-thin film with controlled thickness. Low pressure plasma accelerated chemical vapour deposition of PANI on CNT ensures a regular morphology of PANI in contrast to simple electrochemical deposition, which results in random morphology and narrows the conducting pathways. Vertically aligned CNTs and PANI/CNT electrodes have specific capacitances of 12 F/g and 1225

F/g at 5 mV/s, respectively. In a three-electrode system, the PANI/CNT electrodes demonstrated high cycling stability (65% at 15 A/g after 5800 cycles).

6.3 PANI/Carbon Fiber

Carbon nanofibers (CNFs) are an excellent alternative to CNTs for energy storage devices due to their superior mechanical, electrical, and thermal conductivity properties. Furthermore, they are less expensive, and are simpler to manufacture. There is a lot of interest in developing PANI-CNF composite with superior supercapacitor performance since PANI materials have high specific capacitance and CNFs have a long cycle life. CNFs not only offer shorter electron pathways [45] but also allow ions to enter the fiber from directions perpendicular to its longitudinal axis, which makes them ideal for CNF-based supercapacitors.

Yanilmaz and coworkers [84] used the sol–gel and electrospinning methods to fabricate binder-free flexible PANI/carbon nanofiber electrodes. The hybrid electrode outperformed an individual carbon nanofiber electrode in terms of specific capacitance (234 F/g) and cycling stability (90% after 1000 cycles). In addition, it has a high energy density of 32 Wh/kg at a power density of 500 W/kg. The remarkable pseudocapacitive characteristics of the PANI coating on the carbon nanofiber are responsible for the high performance. The possible reason for poor rate capability of PANI/CNF nanocomposites was the high internal resistance of CNFs carbonized below 1000 °C [45], which led to a negative effect on electron transport and decrease the capacitive behavior of the nanocomposite. The electrical conductivity and hydrophilicity of CNFs should be considered in order to increase the rate capability, graphitized electrospun carbon fibers GECF which carbonized at 2200 °C were immersed in concentrated sulfuric acid for a short time [98]. Then Hou and coworkers [25] used in situ polymerization to grow long, ordered and needle-like PANI nanowires on GECF surface. 3D flexible composite of PANI/GECF electrodes without using any binders and conductive additives presented a high specific capacitance of 976.5 F/g at 0.4 A/g, an energy density approached 86.8 Wh/kg, and a capacitance retention ratio of 89.2% after 1000 cycles at 10 A/g. Furthermore, at a high current density of 50 A/g, PANI/GECF electrodes kept a specific capacitance of about 500 F/g and a coulombic efficiency of 95%.

To achieve the best possible supercapacitive performance and to push the energy density of supercapacitor electrode to a new limit; the active material, electrolyte, and substrate must all be engineered to operate together in a supercapacitor. Hashemi and coworkers [24] fabricated tubular form with rectangular pores of PANI as an active material on chemically functionalized carbon cloth FCC as a substrate as shown in Fig. 7a–b. Then, they added 1,4-napthoquinone (NQ) to the electrolyte as a redox additive, which not only offers pseudo- capacitance through direct redox processes on the electrode surface, but also forms the basis for a regeneration pathway to long-term usage of electrode active materials. After that, asymmetric configuration device used electrolyte of an acidic polymer hydrogel containing the redox additive and made

up of two electrodes PANI/FCC as the positive electrode and negative electrode of AC-FCC as shown in Fig. 7a. In the presence of NQ and at current density of 1.4 A/g, this device exhibited an outstanding specific capacitance of roughly 4007 F/g, which is more than 14.5 times greater than when NQ wasn't present. (Fig. 7c). Furthermore, the device shows extremely high energy density of 1091 Wh/kg, high-power density up to 196 kW/kg, and 84% cycling stability under 35 A/g current density during 7000 cycles Fig. 7d–e. A clock, a red LED, and a rotor were all successfully operated for 1 h and 17 min, 47 min, and more than 20 s, respectively, by two asymmetric devices connected in series. (Fig. 7f).

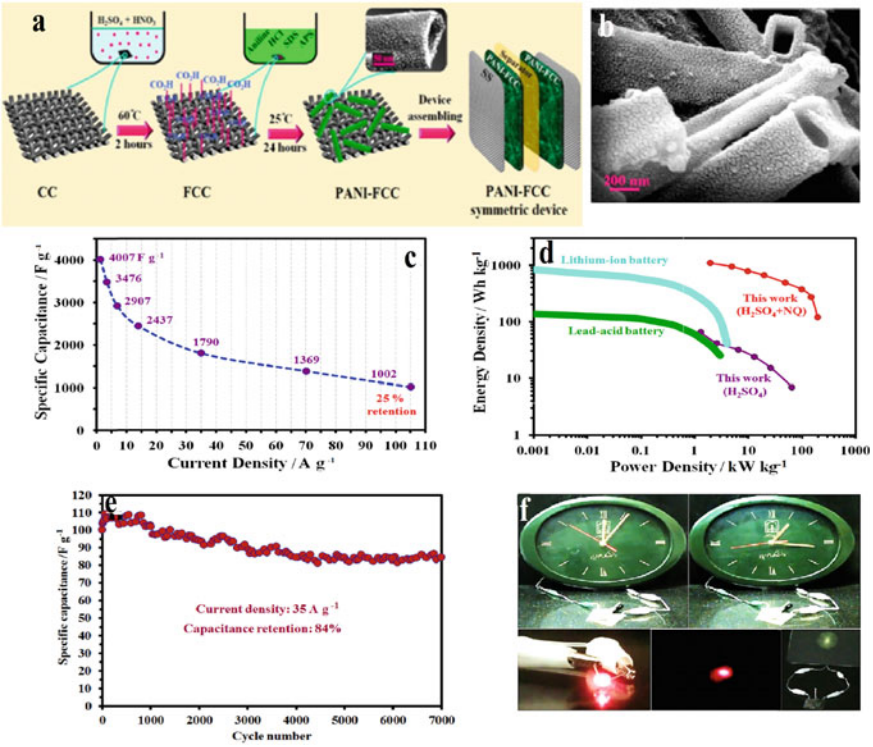

Fig. 7 **a** Schematic design of (PANI-FCC) device. **b** Field emission scanning electron microscope (FE-SEM) images of PANI. **c** estimated capacitance for an AC-FCC//PANI-FCC device from 1.4 to 105 A/g in the presence of napthoquinone NQ as a function of current density. **d** Ragone plots for an asymmetric device at different current densities compared to active mass normalized commercial devices. **e** Cyclability under 35 A/g current density during 7000 cycles; and **f** photographs of running a clock, lighting a red LED and turning a rotor with two asymmetric supercapacitors in series (figure used by permission of Elsevier) [24]

6.4 PANI/Graphene Electrode Materials

Graphene, a one-atomic thick layer of 2-D with unique morphology, was discovered in 2004 by Novoselov and Geim [55] to be a potential electrode material. Graphene has exceptional properties, such as [69]:

- High electrical conductivity (~200 Sm^{-1}),
- Great thermal conductivity (5000 W m^{-1} K^{-1}),
- Large surface area (> 2600 m^2g^{-1}),
- Great charge mobility (> 200,000 cm^2 V^{-1} s^{-1}),
- Excellent chemical and thermal stability,
- Strong Young's modulus (1 TPa); and

Based on the advantages of PANI and graphene that mentioned previously, PANI/graphene nanocomposites have become crucial electrodes for supercapacitors due to the high mechanical stability with a wide thermal operating range and the synergistic effects. On the one hand, homogeneous PANI coating on graphene sheets acts as a spacer to separate nearby graphene sheets, prevent their irreversible aggregation from occurring, and raise the usage ratio, adding more EDL capacitance to the overall capacitance [45]. On the other hand, graphene sheets offer outstanding chemical stability, high surface area, significant increase in electrical conductivity, fast electron/ion transport and a wide working potential in electrochemical devices. These advantages render it as an attractive support material to restrict the volumetric changes (expansion/contraction) and improve the cycle stability of PANI [45]. Depositing a PANI on a graphene electrode without a binder by electrochemical polymerization can overcome the drawbacks of poor stability and high resistance of the powder sample. Ye and coworkers [85] synthesized an ordered PANI nanowire array by electrochemical method on partial exfoliated graphite substrate to produce a hierarchical nanostructure. It effectively reduced the disadvantage of "dead volume" caused by the PANI stacking. Moreover, a pathway for the quick transport of electrons and ions is created by the flawless bonding of the graphene nanosheets and orderly PANI nanowire arrays. Finally, high cycle stability is ensured by the presence of graphene, which reduces the volumetric changes of PANI. A high capacitance of 3.57 F/cm^2 (607 F/g at 1 A/g) and outstanding cycling stability (80.4% after 10,000 GCD cycles) were displayed by the ordered PANI nanowire and the graphene network [85]. Adding functional groups and vacancy defects to the graphene surface provide a great beneficial in energy storage mechanism. By enriching the active sites of graphene, the specific capacitance and cycling stability of PANI/graphene composites may be greatly enhanced. Zheng and coworkers [96] developed a route for the preparation of a high electrochemical performance electrode based on three-dimensional multi-growth site graphene MSG/PANI nanocomposite. Active sites on the surface of graphene nanosheets, such as oxygen functional groups and carbon vacancy defects, were produced using chemical treatment (70% HNO_3 and 30%H_2O_2). MSG/PANI nanocomposites were found to have a specific capacitance of 912 F/g at 1 A/g, which is much greater than GO/PANI without acid treatment (432 F/g), maximum specific

energy and maximum specific power of 30 Wh/kg and 3200 W/kg, respectively. The capacitance retention rate of the nanocomposite achieved 86.4% at a high current density of 20 A/g, and after 10,000 GCD cycles at 10 A/g, it attained 89.5% cycle stability. Tabrizi and coworkers [68] found that an acid-treated GO/PANI nanocomposite with a porous structure and high specific surface area revealed a maximum capacitance of 727 F/g which attributed to acid functionalization and well-defined PANI nanoarrays on GO sheets. The symmetrical device designed by combining these electrodes has a maximum energy density of 40 Wh/kg and a power density of up to 15.3 kW/kg with an outstanding stability (95.7% retention after 5000 cycles). Li and coworkers [39] used a supra-molecular in-situ assembly approach to decorate carbon nanodots on graphene-PANI (rGO@CN/PANI). The nanocomposites reveal high electrochemical performance with specific capacitance of 871.8 F/g at 0.2A/g and acceptable cycling performance (72% after 10,000 CV cycles at 30 mV/s). Mangisetti and coworkers [52] prepared nitrogen doped 3D porous carbon-graphene/PANI (3D PC-g/PANI) by a simple in-situ polymerization process. They also synthesized N-doped porous carbon/gC_3N_4 from bio- waste seeds to use as a negative electrode for ASC device. The 3D porous carbon prevents graphene nanosheets from aggregating and produces a 3D PC-g composite with a well-connected structure, that provides high conductivity, quick ion and charge transport, and high surface area (2418 m^2/g). Also, more space can be provided when using 3D PC-g as a template for PANI dispersion, which minimized the volumetric changes of PANI through charging and discharging cycles. In 0.5 M Na_2SO_4 electrolyte, symmetric SC device of 3D PC-g/PANI shows a high energy density of 117 Wh/kg and retained about 94% of initial capacitance. Also, The ASC device offered a high electrochemical performance with energy density of 97.5 Wh/kg and cyclic stability of up to 91% after 10,000 cycles in 0.5 M Na_2SO_4 as shown in Fig. 8. Table 4 lists some recent studies on graphene/PANI composites.

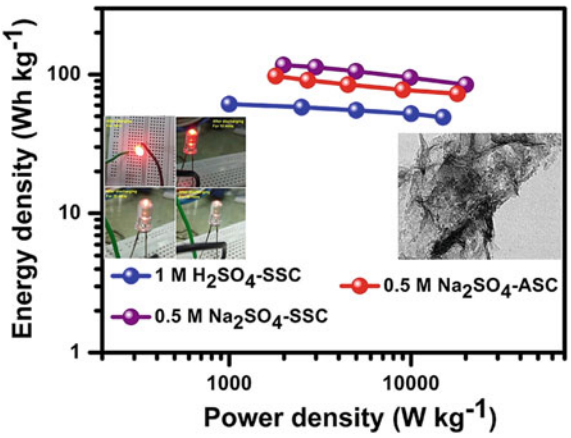

Fig. 8 Ragone plot of 3D N-doped porous carbon-graphene/Polyaniline nanohybrid as a function of current densities in different electrolytes for SSC and ASC (figure used by permission of Elsevier) [52]

Table 4 Various supercapacitor electrode materials based on graphene and PANI nanocomposites

Nanocomposite	Electrolyte	Substrate	Specific capacitance	Capacitance retention	Refs.
Graphene/PANI layers/PANI nanorods	1 M H_2SO_4	Glass carbon	578 F/g at 1 A/g	93% after 10,000 cycles at 2 A/g	[38]
PANI nanofibers/rGO	1 M H_2SO_4	Stainless steel mesh	692 F/g at 1A/g	83.3% after 1,000 cycles at 10 A/g	[32]
Flower-like PANI/graphene hybrid	1 M H_2SO_4	Glassy carbon	1510 F/g at 1 A/g	89% after 1,500 cycles at 100 mV/s	[33]
Sulfonated PANI/GO	1 M H_2SO_4	Glassy carbon	1107 F/g at 1 A/g	94% after 5,000 cycles at 3.8 A/g	[2]
Phytic acid assisted graphene/PANI	1 M H_2SO_4	Glassy carbon	865.6 F/g at 1 A/g	82% after 1,000 cycles at 5 A/g	[31]
PANI/rGO	1 M H_2SO_4	Pt foil	423 F/g at 0.8 A/g	75% after 1,000 cycles at 50 mA/cm^2	[76]
Graphene carbon sphere/PANI/rGO	1 M H_2SO_4	Stainless steel mesh	446 F/g at 5 mV/s	88.7% after 5,000 cycles at 2 A/g	[43]
Holey N-doped rGO/PANI	1 M H_2SO_4	Slice of carbon	746 F/g at 1 A/g	97% after 2000 cycles at 100 mV/s	[42]
3D rGO/self-suspended PANI	1 M H_2SO_4	glassy carbon	480 F/g at 1 A/g	94.16% after 10,000 cycles at 10 A/g	[16]
N-doped graphene/PANI hydrogels	1 M H_2SO_4	Stainless steel mesh	514.3 F/g at 1 A/g	87.1% after 1,000 cycles at 10 A/g	[99]
PANI nanorod arrays/graphene	1 M H_3PO_4	Graphene fiber	0.23 F/cm^2 at 0.1 mA/cm^2	86.9% after 8,000 cycles at 0.8 mA/cm^2	[78]
PANI/rGO/functionalized carbon cloth	1 M H_2SO_4	Carbon cloth	0.47 F/cm^2 at 0.5 mA/cm^2	75.5% after 10,000 cycles at 0.8 mA/cm^2	[13]
GO/PANI/Ni(OH)2	6 M KOH	Nickel foam	743 F/g at 1 mV/s	84.4% after 2,000 cycles at 20 mA/cm^2	[48]
Graphene/MnO_2/PANI	6 M KOH	Nickel foam	1081 F/g at 1 mV/s	99% after 1,000 cycles at 3 A/g	[70]

(continued)

Table 4 (continued)

Nanocomposite	Electrolyte	Substrate	Specific capacitance	Capacitance retention	Refs.
PGO@PANI	6 M KOH	Nickel foam	603 F/g at 1 A/g	77% after 1,500 cycles at 3 A/g	[4]

6.5 PANI/Graphene Quantum Dots Electrode Materials

The chemical interaction can introduce graphene quantum dots as a molecule dopant into PANI chains. The graphene quantum dots GQDs did not only offer the double-layer properties to the nanocomposites, but it also improved the charge transfer to the surface of PANI. Malik and coworkers [54] prepared GQDs from graphene oxide flakes, followed by synthesis GQD-PANI by the chemical oxidation method of aniline. The synthesized GQD-PANI composites show a specific capacitance of 1044 F/g at 1 A/g with 80.1% cyclic stability after 3000 cycles and this high specific capacitance is attributed to higher surface areas in nanotube morphology which provide better conductive paths for fast electron transportation. In previous studies our group showed that the Sulfur and nitrogen co-doped GQDs has a positive impact on the electrochemical properties of PANI. PANI/S,N:GQDs nanocomposite exhibited maximum specific capacitance of 2524 F/g at 2 A/g with an excellent cyclic stability of 100% after 1000 cycles [60].

7 PANI/Metal Compounds

Because of their potential for pseudocapacitance over a large range of potential and excellent stability, metal compounds are interesting candidates for supercapacitors. However, they typically have limited electrical conductivity. In recent years, the nanocomposites of PANI with high conductivity and metal compounds such as Metal oxides/hydroxide, metal sulfides, metal chlorides, and metal nitrides have all been employed as supercapacitor electrodes to improve electrochemical performance.

Metal oxides/hydroxides (MOx) electrode materials are characterized as Faradaic pseudocapacitive materials. In general, they offer higher energy density than carbon-based materials and better electrochemical stability than conducting polymers for supercapacitors [66]. The following general conditions must be satisfied before using metal oxide in supercapacitors.

(i) High specific surface area.
(ii) Electrical conductivity.
(iii) Possibility of existing in two or more oxidation states across continuous range without phase transitions; and

Among the metal oxides, RuO_2, MnO_2, V_2O_5, cobalt oxide/hydroxide, nickel oxide/hydroxide, etc. have been investigated as electrode materials for supercapacitors applications. Due to its wide working potential window, highly reversible redox processes, and three different oxidation states, RuO_2 is the most researched metal oxide. Additionally, RuO_2 has a high specific capacitance (900 F/g), metallic conductivity, good thermal stability, and extended cycle life. However, the poor performance at high current densities, toxicity, and high cost limit practical applications of RuO_2-based supercapacitors.

MnO_2, on the other hand, has a large theoretical specific capacitance (1370 F/g), is inexpensive, and is environmentally friendly, but its poor conductivity restricts its applicability [3, 79] Considering these facts, constructing a MnO_2/PANI composite is a suitable way to increase the electrochemical use of MnO_2 and PANI in supercapacitors. PANI/MnO_2 composites have been synthesized electrochemically via pulse electrodeposition by Liu and coworkers [46]. The prepared composite has rod-like structure and MnO_2 particles were uniformly distributed on PANI nanorod. MnO_2 and PANI work together synergistically to produce MnO_2/PANI composite with higher specific capacitance (810 F/g) than pure PANI (662 F/g) at 0.5 A/g. Also, after 1000 cycles, it maintained 86.3% of its original capacitance. The electrochemical properties of PANI/MnO_2 composite were studied extensively in recent years. However, it suffers from poor contact between MnO_2 and PANI membrane restricts the complete interface of electrolyte and MnO_2 resulting the loss in energy density. A super bridge between the PANI membrane and the MnO_2 nanostructure is required. The MnO_2/PANI composite with silver nanoparticle decoration has a higher specific capacitance and superior conductivity. Silver nanoparticle not only facilitate the electron transfer but also reduce the internal resistance of metal oxide pseudocapacitive materials and increase the proton diffusion throughout the electrodes [57]. Among metal oxides, double metal oxides have attracted attention for electrochemical energy storage due to their ability to create multiple oxidation states and electrical conductivity in ways that single metal oxides and carbon-based materials cannot [5]. Yu and coworkers [87] showed that the core of $NiCo_2O_4$ nanowires has strong electrical conductivity and may be used as a backbone and electron highway for charge storage, overcoming MnO_2's low electrical conductivity. In the core–shell structure, the $NiCo_2O_4$ core was also employed to improve the structural instability of PANI. Jabeen and coworkers [30] provided a new method for fabricating a core–shell $NiCo_2O_4$/PANI nanorod arrays for high stability PANI based-electrode material for SCs as illustrated in Fig. 9a. Highly porous conductive core $NiCo_2O_4$ not only acts as a strain buffer support for PANI layer but also offers rapid electron transport pathways between PANI and current collector, resulting in small electrode polarization and great power capability. The heterostructure achieves a high specific capacitance of 901 F/g at 1 A/g, exceptional cycling stability of ~91% after 3000 GCD cycles at 10 A/g and good coulombic efficiency shown in Fig. 9b.

Transition metal molybdates, such as $MnMoO_4$, $CoMoO_4$, and $NiMoO_4$, with superior pseudocapacitive characteristics have developed as promising electrode materials in recent years [50]. For example, Liu and coworkers [44] reported a facile

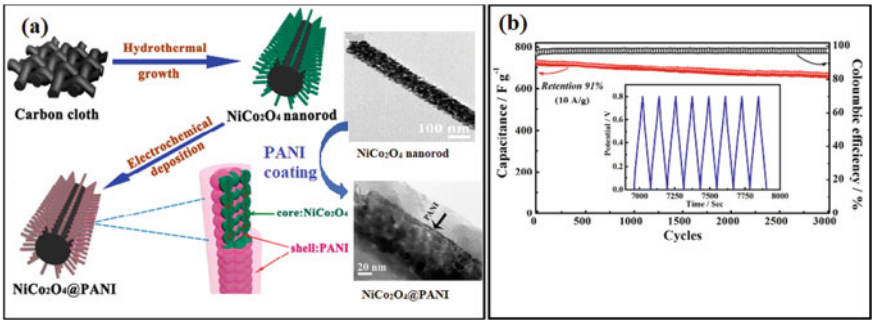

Fig. 9 **a** Schematic diagram of the fabrication process for $NiCo_2O_4$@PANI nanorod arrays. **b** Cycle performance of the $NiCo_2O_4$@PANI nanorod arrays electrode for 3000 successive charge–discharge cycles at a large current density of 10 A/g and corresponding Coulombic efficiency (inset is the typical charge–discharge curves). Reprinted with permission from [30], copyright (2016) American Chemical Society

method for fabricating $CoMoO_4$-$NiMoO_4$. xH_2O bundles with a high specific capacitance but poor cycle life (only 75.1% of the initial specific capacitance remained after 1000 GCD cycles). The structural collapse of $NiMoO_4$ during charge and discharge operations might be prevented by PANI with high mechanical stability. As a result of the synergistic effect between them, PANI/$NiMoO_4$ nanocomposite exhibited high capacitance retention of 80.7% after 2000 cycles at 5 A/g, and high specific capacitance of 1214 F/g at 1 A/g, revealing their good electrochemical stability [15].

Tungsten oxide (WO_3) has gained popularity as a viable SC electrode material in recent years due to its large specific surface area, electrochemical stability, and environmental friendliness [95]. However, low capacitance of WO_3 limit its application in high performance pseudocapacitor. WO3 modified with PANI has attracted a lot of attention for enhancing specific capacitance and cycle stability due to the synergistic effects of each component. Yang and coworkers [83] fabricated the inner/outer coating structural hexagonal WO_3/PANI through the hydrothermal-electrodeposition route. The hexagonal WO_3 nanowires were grown-up on the titanium Ti surface, and the outer PANI layer decorates the inner WO_3, resulting in WO_3-PANI hybrid nanostructures as shown in Fig. 10a. The specific capacitance (278 F/g at 1 A/g) and good cycle stability (91.9% after 1500 cycles) of WO_3/PANI electrode Fig. 10b should be attributed to its innovative nanostructure design and the interaction between the outer PANI layer with the inner WO_3 layer. On the one hand, PANI could dramatically increase the capacitance of hybrid electrodes, which is due to two factors: high specific capacitance and excellent electrical properties. On the other hand, the free spaces within the porous hexagonal-WO3 interior helps the volumetric expansion of PANI during charge and discharge cycling.

Recently, Metal tungstates such as $CoWO_4$ [7], $ZnWO_4$ [20], $MnWO_4$ [58], $FeWO_4$ [19], and $CuWO_4$ [36] are regarded the most attractive transition-metal oxides due to low toxicity, abundance, rich polymorphism, and stable multifunctional

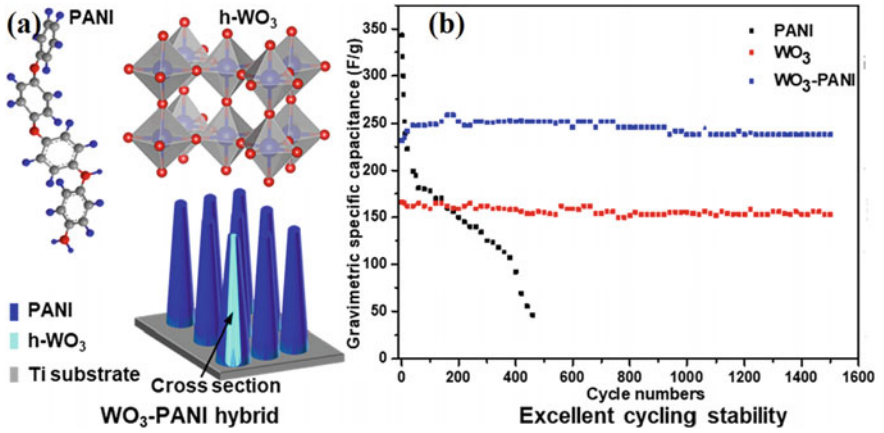

Fig. 10 **a** Schematic illustration of h-WO3/PANI hybrid nanostructures. **b** Cycling performance of the PANI, WO3, and WO3/PANI at a current density of 3 A/g, respectively (figure used by permission of Elsevier) [83]

properties. CoWO4/PANI electrode exhibited high specific capacitance of 653 F/g and outstanding cycling stability of 93.3% even after 5000 GCD cycles [59].

Supercapacitor electrode materials can also be made of other metal compounds, such as metal sulfides, metal chlorides, and metal nitrides. They are more stable in acidic electrolytes than metal oxides, but they lack the electrical conductivity and electrochemical performance of metal oxides. Majhi and coworkers [51] synthesized PANI/$CoCl_2$ composites through in situ polymerization process with different doping levels of CoCl2 (10, 15 and 20 wt%). The CV test revealed that the PANI–10% $CoCl_2$ composite had a significantly higher specific capacitance value (918 F/g) than pure PANI (382 F/g). This shows that the electrochemical performance of PANI–10% $CoCl_2$ is significantly influenced by the quantity of $CoCl_2$ present in the composite.

Because of its unique structural features and larger theoretical capacitance (than graphite 2D molybdenum disulfide MoS_2 nanosheets have increasingly attracted a lot of attention in the fields of energy storage. MoS_2 monolayers are made up of three atom layers (S-Mo-S), and their adaptability can be related to the analogous structure of graphene, which can provide a large surface area. Unfortunately, 2D MoS_2 nanosheets are easy to agglomerate due to the strong interlayer van der Waals forces [62], resulting in a decrease in active surface area and poor specific capacitance. The combination of conductive PANI with molybdenum disulfide MoS_2 not only prevents 2D MoS_2 nanosheet agglomeration, but also improves PANI cycle stability, which is beneficial to their electrochemical abilities [28]. Zhao and coworkers [94] have created a highly conductive metallic MoS_2 and PANI monolayers with unique alternating heterostructure, which will help to enhance electron/ion transfer across the electrode material while also providing great structural stability (91% capacitance retention after 2000 cycles). Zhang and coworkers [92] investigate the MoS_2/PANI core–shell structure (Fig. 11) as a supercapacitor electrode. This pompon- shaped

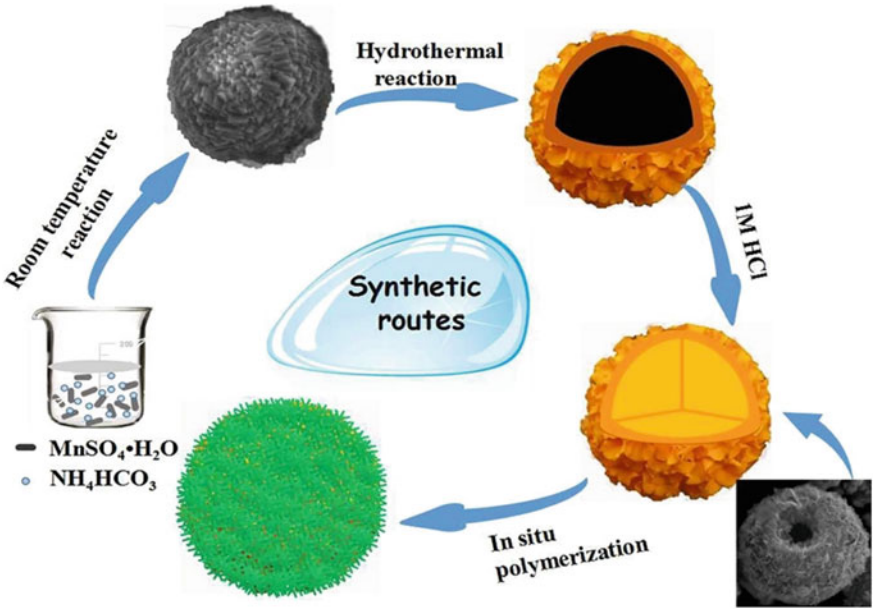

Fig. 11 Schematic illustration of the formation of MoS_2/PANI core/shell microsphere (figure used by permission of Elsevier) [92]

MoS_2/PANI composites with a high specific surface area and a more mesoporous pores presented a specific capacitance of 633 F/g with cycle stability of 86% for 1000 cycles.

Among the metal nitrides, Titanium nitrides (TiN) has an excellent candidate as an electrode material for SCs in highly corrosive electrolytes [12] due to its corrosion resistance, low-cost, thermal stability, mechanical properties and good electrical conductivity [82, 97]. Xia and coworkers [80] prepared a PANI/TiN core–shell nanowire arrays (NWAs) by electrodepositing PANI onto TiN NWAs. The TiN NWAs core was vital in improving the electrode's rate performance by providing a large surface area and rapid electron transport. The PANI shell on TiN NWAs might improve cycle stability and help to achieve excellent pseudo-capacitance performance. The PANI/TiN core–shell NWAs electrode exhibited a very high specific capacitance of 1064 F/g at 1A/g and kept 95% capacity retention after 200 cycles.

8 Conclusion

This chapter summarized current developments in PANI as a supercapacitor electrode material, including their design, and synthesis process. Pure PANI is unable to fulfil the rising demand due to its poor cycling stability and inefficient capacitance

contribution. As a result, PANI must be used in conjunction with other active materials such as carbon materials and metal compounds. Due to the synergistic effect, PANI works as a conductive layer in various PANI based composite structures, and the resulting PANI based composites have showed improved electrochemical performance in supercapacitors.

References

1. Ali F, Liu X, Zhou D, Yang X, Xu J, Schenk T, Müller J, Schroeder U, Cao F, Dong X (2017) Silicon-doped hafnium oxide anti-ferroelectric thin films for energy storage. J Appl Phys 122(14):144105. https://doi.org/10.1063/1.4989908
2. Bandyopadhyay P, Kuila T, Balamurugan J, Nguyen TT, Kim NH, Lee JH (2017) Facile synthesis of novel sulfonated polyaniline functionalized graphene using m-aminobenzene sulfonic acid for asymmetric supercapacitor application. Chem Eng J 308:1174–1184. https://doi.org/10.1016/j.cej.2016.10.015
3. Bélanger D, Brousse T, Long J (2008) Manganese oxides: battery materials make the leap to electrochemical capacitors. Electrochem Soc Interface 17(1):49–52. https://doi.org/10.1149/2.f07081if
4. Bigdeli H, Moradi M, Borhani S, Jafari EA, Hajati S, Kiani MA (2018) One-pot electrochemical growth of sponge-like polyaniline-intercalated phosphorous-doped graphene oxide on nickel foam as binder-free electrode material of supercapacitor. Phys E 100:45–53. https://doi.org/10.1016/j.physe.2018.03.003
5. Cai D, Wang D, Liu B, Wang Y, Liu Y, Wang L, Li H, Huang H, Li Q, Wang T (2013) Comparison of the electrochemical performance of $NiMoO_4$ nanorods and hierarchical nanospheres for supercapacitor applications. ACS Appl Mater Interfaces 5(24):12905–12910. https://doi.org/10.1021/am403444v
6. Cao Z, Wei B (2013) A perspective: carbon nanotube macro-films for energy storage. Energy Environ Sci 6(11):3183–3201. https://doi.org/10.1039/C3EE42261E
7. Chen S, Yang G, Jia Y, Zheng H (2016) Facile synthesis of CoWO4 nanosheet arrays grown on nickel foam substrates for asymmetric supercapacitors. ChemElectroChem 3(9):1490–1496. https://doi.org/10.1002/celc.201600316
8. Chen W, Rakhi RB, Alshareef HN (2013) Morphology-dependent enhancement of the pseudocapacitance of template-guided tunable polyaniline nanostructures. J Phys Chem C 117(29):15009–15019. https://doi.org/10.1021/jp405300p
9. Conway BE (1991) Transition from "supercapacitor" to "battery" behavior in electrochemical energy storage. J Electrochem Soc 138(6):1539–1548
10. Dhawale DS, Dubal DP, Jamadade VS, Salunkhe RR, Lokhande CD (2010a) Fuzzy nanofibrous network of polyaniline electrode for supercapacitor application. Synth Met 160(5):519–522. https://doi.org/10.1016/j.synthmet.2010.01.021
11. Dhawale DS, Salunkhe RR, Jamadade VS, Dubal DP, Pawar SM, Lokhande CD (2010b) Hydrophilic polyaniline nanofibrous architecture using electrosynthesis method for supercapacitor application. Curr Appl Phys 10(3):904–909. https://doi.org/10.1016/j.cap.2009.10.020
12. Dong S, Chen X, Gu L, Zhou X, Li L, Liu Z, Han P, Xu H, Yao J, Wang H, Zhang X, Shang C, Cui G, Chen L (2011) One dimensional MnO_2/titanium nitride nanotube coaxial arrays for high performance electrochemical capacitive energy storage. Energy Environ Sci 4(9):3502–3508. https://doi.org/10.1039/C1EE01399H
13. Du P, Dong Y, Kang H, Yang X, Wang Q, Niu J, Wang S, Liu P (2018) Graphene-wrapped polyaniline nanowire array modified functionalized of carbon cloth for high-performance flexible solid-state supercapacitor. ACS Sustain Chem Eng 6(11):14723–14733. https://doi.org/10.1021/acssuschemeng.8b03278

14. Eftekhari A, Li L, Yang Y (2017) Polyaniline supercapacitors. J Power Sources 347:86–107. https://doi.org/10.1016/j.jpowsour.2017.02.054
15. Gao H, Wu F, Wang X, Hao C, Ge C (2018) Preparation of $NiMoO_4$-PANI core-shell nanocomposite for the high-performance all-solid-state asymmetric supercapacitor. Int J Hydrogen Energy 43(39):18349–18362. https://doi.org/10.1016/j.ijhydene.2018.08.018
16. Gao Z, Yang J, Huang J, Xiong C, Yang Q (2017) A three-dimensional graphene aerogel containing solvent-free polyaniline fluid for high performance supercapacitors. Nanoscale 9(45):17710–17716. https://doi.org/10.1039/C7NR06847F
17. Gawli Y, Banerjee A, Dhakras D, Deo M, Bulani D, Wadgaonkar P, Shelke M, Ogale S (2016) 3D polyaniline architecture by concurrent inorganic and organic acid doping for superior and robust high rate supercapacitor performance. Sci Rep 6:21002. https://doi.org/10.1038/srep21002. https://www.nature.com/articles/srep21002#supplementary-information
18. Ghenaatian HR, Mousavi MF, Rahmanifar MS (2012) High performance hybrid supercapacitor based on two nanostructured conducting polymers: Self-doped polyaniline and polypyrrole nanofibers. Electrochim Acta 78:212–222
19. Goubard-Bretesché N, Crosnier O, Buvat G, Favier F, Brousse T (2016) Electrochemical study of aqueous asymmetric $FeWO_4/MnO_2$ supercapacitor. J Power Sources 326:695–701. https://doi.org/10.1016/j.jpowsour.2016.04.075
20. Guan B, Hu L, Zhang G, Guo D, Fu T, Li J, Duan H, Li C, Li Q (2014) Facile synthesis of ZnWO 4 nanowall arrays on Ni foam for high performance supercapacitors. RSC Adv 4(9):4212–4217
21. Guan H, Fan L-Z, Zhang H, Qu X (2010) Polyaniline nanofibers obtained by interfacial polymerization for high-rate supercapacitors. Electrochim Acta 56(2):964–968. https://doi.org/10.1016/j.electacta.2010.09.078
22. Gupta V, Miura N (2005) Electrochemically deposited polyaniline nanowire's network a high-performance electrode material for redox supercapacitor. Electrochem Solid-State Lett 8(12):A630–A632
23. Hadjipaschalis I, Poullikkas A, Efthimiou V (2009) Overview of current and future energy storage technologies for electric power applications. Renew Sustain Energy Rev 13(6):1513–1522. https://doi.org/10.1016/j.rser.2008.09.028
24. Hashemi M, Rahmanifar MS, El-Kady MF, Noori A, Mousavi MF, Kaner RB (2018) The use of an electrocatalytic redox electrolyte for pushing the energy density boundary of a flexible polyaniline electrode to a new limit. Nano Energy 44:489–498. https://doi.org/10.1016/j.nanoen.2017.11.058
25. He S, Hu X, Chen S, Hu H, Hanif M, Hou H (2012) Needle-like polyaniline nanowires on graphite nanofibers: hierarchical micro/nano-architecture for high performance supercapacitors. J Mater Chem 22(11):5114–5120. https://doi.org/10.1039/C2JM15668G
26. Holdren JP (1991) Population and the energy problem. Popul Environ 12(3):231–255. https://doi.org/10.1007/BF01357916
27. Huang H, Zeng X, Li W, Wang H, Wang Q, Yang Y (2014) Reinforced conducting hydrogels prepared from the in situ polymerization of aniline in an aqueous solution of sodium alginate. J Mater Chem A 2(39):16516–16522. https://doi.org/10.1039/C4TA03332A
28. Huang K-J, Wang L, Liu Y-J, Wang H-B, Liu Y-M, Wang L-L (2013) Synthesis of polyaniline/2-dimensional graphene analog MoS_2 composites for high-performance supercapacitor. Electrochim Acta 109:587–594. https://doi.org/10.1016/j.electacta.2013.07.168
29. Hussain S, Kovacevic E, Amade R, Berndt J, Pattyn C, Dias A, Boulmer-Leborgne C, Ammar M-R, Bertran-Serra E (2018) Plasma synthesis of polyaniline enrobed carbon nanotubes for electrochemical applications. Electrochim Acta 268:218–225. https://doi.org/10.1016/j.electacta.2018.02.112
30. Jabeen N, Xia Q, Yang M, Xia H (2016) Unique core-shell nanorod arrays with polyaniline deposited into mesoporous $NiCo_2O_4$ support for high-performance supercapacitor electrodes. ACS Appl Mater Interfaces 8(9):6093–6100. https://doi.org/10.1021/acsami.6b00207
31. Ji J, Li R, Li H, Shu Y, Li Y, Qiu S, He C, Yang Y (2018) Phytic acid assisted fabrication of graphene/polyaniline composite hydrogels for high-capacitance supercapacitors. Compos B Eng 155:132–137. https://doi.org/10.1016/j.compositesb.2018.08.037

32. Jin K, Zhang W, Wang Y, Guo X, Chen Z, Li L, Zhang Y, Wang Z, Chen J, Sun L, Zhang T (2018) In–situ hybridization of polyaniline nanofibers on functionalized reduced graphene oxide films for high-performance supercapacitor. Electrochim Acta 285:221–229. https://doi.org/10.1016/j.electacta.2018.07.220
33. Ke F, Liu Y, Xu H, Ma Y, Guang S, Zhang F, Lin N, Ye M, Lin Y, Liu X (2017) Flower-like polyaniline/graphene hybrids for high-performance supercapacitor. Compos Sci Technol 142:286–293. https://doi.org/10.1016/j.compscitech.2017.02.026
34. Kolathodi MS, Palei M, Natarajan TS, Singh G (2020) MnO_2 encapsulated electrospun TiO_2 nanofibers as electrodes for asymmetric supercapacitors. Nanotechnology 31(12):125401. https://doi.org/10.1088/1361-6528/ab5d64
35. Kulandaivalu S, Sulaiman Y (2020) Review of the use of transition-metal-oxide and conducting polymer-based fibres for high-performance supercapacitors. Mater Des 186:108199
36. Kumar RD, Karuppuchamy S (2014) Microwave-assisted synthesis of copper tungstate nanopowder for supercapacitor applications. Ceram Int 40(8):12397–12402
37. Li G-R, Feng Z-P, Zhong J-H, Wang Z-L, Tong Y-X (2010a) Electrochemical synthesis of polyaniline nanobelts with predominant electrochemical performances. Macromolecules 43(5):2178–2183. https://doi.org/10.1021/ma902317k
38. Li J, Xiao D, Ren Y, Liu H, Chen Z, Xiao J (2019a) Bridging of adjacent graphene/polyaniline layers with polyaniline nanofibers for supercapacitor electrode materials. Electrochim Acta 300:193–201. https://doi.org/10.1016/j.electacta.2019.01.089
39. Li S, Gao A, Yi F, Shu D, Cheng H, Zhou X, He C, Zeng D, Zhang F (2019b) Preparation of carbon dots decorated graphene/polyaniline composites by supramolecular in-situ self-assembly for high-performance supercapacitors. Electrochim Acta 297:1094–1103. https://doi.org/10.1016/j.electacta.2018.12.036
40. Li X, Li X, Dai N, Wang G, Wang Z (2010b) Preparation and electrochemical capacitance performances of super-hydrophilic conducting polyaniline. J Power Sources 195(16):5417–5421. https://doi.org/10.1016/j.jpowsour.2010.03.034
41. Li X, Wei B (2013) Supercapacitors based on nanostructured carbon. Nano Energy 2(2):159–173. https://doi.org/10.1016/j.nanoen.2012.09.008
42. Liu J, Du P, Wang Q, Liu D, Liu P (2019a) Mild synthesis of holey N-doped reduced graphene oxide and its double-edged effects in polyaniline hybrids for supercapacitor application. Electrochim Acta 305:175–186. https://doi.org/10.1016/j.electacta.2019.03.049
43. Liu L, Wang Y, Meng Q, Cao B (2017) A novel hierarchical graphene/polyaniline hollow microsphere as electrode material for supercapacitor applications. J Mater Sci 52(13):7969–7983. https://doi.org/10.1007/s10853-017-1000-2
44. Liu MC, Kong LB, Lu C, Ma XJ, Li XM, Luo YC, Kang L (2013) Design and synthesis of CoMoO4-NiMoO4·xH 2O bundles with improved electrochemical properties for supercapacitors. J Mater Chem A 1(4):1380–1387. https://doi.org/10.1039/c2ta00163b
45. Liu P, Yan J, Guang Z, Huang Y, Li X, Huang W (2019b) Recent advancements of polyaniline-based nanocomposites for supercapacitors. J Power Sources 424:108–130. https://doi.org/10.1016/j.jpowsour.2019.03.094
46. Liu T, Shao G, Ji M, Wang G (2015) Polyaniline/MnO_2 composite with high performance as supercapacitor electrode via pulse electrodeposition. Polym Compos 36(1):113–120. https://doi.org/10.1002/pc.22919
47. Lokhande VC, Lokhande AC, Lokhande CD, Kim JH, Ji T (2016) Supercapacitive composite metal oxide electrodes formed with carbon, metal oxides and conducting polymers. J Alloy Compd 682:381–403. https://doi.org/10.1016/j.jallcom.2016.04.242
48. Ma L, Su L, Zhang J, Zhao D, Qin C, Jin Z, Zhao K (2016) A controllable morphology GO/PANI/metal hydroxide composite for supercapacitor. J Electroanal Chem 777:75–84. https://doi.org/10.1016/j.jelechem.2016.07.033
49. Ma Y, Hou C, Zhang H, Qiao M, Chen Y, Zhang H, Zhang Q, Guo Z (2017) Morphology-dependent electrochemical supercapacitors in multi-dimensional polyaniline nanostructures. J Mater Chem A 5(27):14041–14052. https://doi.org/10.1039/C7TA03279J

50. Mai LQ, Yang F, Zhao YL, Xu X, Xu L, Luo YZ (2011) Hierarchical MnMoO(4)/CoMoO(4) heterostructured nanowires with enhanced supercapacitor performance. Nat Commun 2:381. https://doi.org/10.1038/ncomms1387
51. Majhi M, Choudhary RB, Thakur AK, Omar FS, Duraisamy N, Ramesh K, Ramesh S (2018) CoCl2-doped polyaniline composites as electrode materials with enhanced electrochemical performance for supercapacitor application. Polym Bull 75(4):1563–1578. https://doi.org/10.1007/s00289-017-2112-1
52. Mangisetti SR, Kamaraj M, Ramaprabhu S (2019) N-doped 3D porous carbon-graphene/polyaniline hybrid and N-doped porous carbon coated gC3N4 nanosheets for excellent energy density asymmetric supercapacitors. Electrochim Acta 305:264–277. https://doi.org/10.1016/j.electacta.2019.03.043
53. Molapo KM, Ndangili PM, Ajayi RF, Mbambisa G, Mailu SM, Njomo N, Masikini M, Baker P, Iwuoha EI (2012) Electronics of conjugated polymers (I): polyaniline. Int J Electrochem Sci 7(12):11859–11875
54. Mondal S, Rana U, Malik S (2015) Graphene quantum dot-doped polyaniline nanofiber as high performance supercapacitor electrode materials. Chem Commun 51(62):12365–12368. https://doi.org/10.1039/C5CC03981A
55. Novoselov KS, Geim AK, Morozov SV, Jiang D, Zhang Y, Dubonos SV, Grigorieva IV, Firsov AA (2004) Electric field effect in atomically thin carbon films. Science 306(5696):666. https://doi.org/10.1126/science.1102896
56. Ozoemena KI, Chen S (2016) Nanomaterials in advanced batteries and supercapacitors. Springer
57. Poudel MB, Shin M, Kim HJ (2021) Polyaniline-silver-manganese dioxide nanorod ternary composite for asymmetric supercapacitor with remarkable electrochemical performance. Int J Hydrogen Energy 46(1):474–485. https://doi.org/10.1016/j.ijhydene.2020.09.213
58. Raj BGS, Acharya J, Seo M-K, Khil M-S, Kim H-Y, Kim B-S (2019) One-pot sonochemical synthesis of hierarchical MnWO4 microflowers as effective electrodes in neutral electrolyte for high performance asymmetric supercapacitors. Int J Hydrogen Energy 44(21):10838–10851. https://doi.org/10.1016/j.ijhydene.2019.03.035
59. Rajkumar S, Christy Ezhilarasi J, Saranya P, Princy Merlin J (2022) Fabrication of CoWO4/PANI composite as electrode material for energy storage applications. J Phys Chem Solids 162:110500. https://doi.org/10.1016/j.jpcs.2021.110500
60. Ramadan A, Anas M, Ebrahim S, Soliman M, Abou-Aly A (2020a) Effect of co-doped graphene quantum dots to polyaniline ratio on performance of supercapacitor. J Mater Sci Mater Electron 31(9):7247–7259. https://doi.org/10.1007/s10854-020-03297-8
61. Ramadan A, Anas M, Ebrahim S, Soliman M, Abou-Aly AI (2020b) Polyaniline/fullerene derivative nanocomposite for highly efficient supercapacitor electrode. Int J Hydrogen Energy. https://doi.org/10.1016/j.ijhydene.2020.04.093
62. Ramakrishna Matte HSS, Gomathi A, Manna AK, Late DJ, Datta R, Pati SK, Rao CNR (2010) MoS2 and WS2 analogues of graphene. Angew Chem Int Ed 49(24):4059–4062
63. Raza W, Ali F, Raza N, Luo Y, Kim K-H, Yang J, Kumar S, Mehmood A, Kwon EE (2018) Recent advancements in supercapacitor technology. Nano Energy 52:441–473. https://doi.org/10.1016/j.nanoen.2018.08.013
64. Sharma V, Sahoo A, Sharma Y, Mohanty P (2015) Synthesis of nanoporous hypercrosslinked polyaniline (HCPANI) for gas sorption and electrochemical supercapacitor applications. RSC Adv 5(57):45749–45754. https://doi.org/10.1039/C5RA03016A
65. Sk MM, Yue CY (2014) Synthesis of polyaniline nanotubes using the self-assembly behavior of vitamin C: a mechanistic study and application in electrochemical supercapacitors. J Mater Chem A 2(8):2830–2838. https://doi.org/10.1039/c3ta14309k
66. Sk MM, Yue CY, Ghosh K, Jena RK (2016) Review on advances in porous nanostructured nickel oxides and their composite electrodes for high-performance supercapacitors. J Power Sources 308:121–140. https://doi.org/10.1016/j.jpowsour.2016.01.056
67. Sumboja A, Wang X, Yan J, Lee PS (2012) Nanoarchitectured current collector for high rate capability of polyaniline based supercapacitor electrode. Electrochim Acta 65:190–195. https://doi.org/10.1016/j.electacta.2012.01.046

68. Tabrizi AG, Arsalani N, Mohammadi A, Ghadimi LS, Ahadzadeh I, Namazi H (2018) A new route for the synthesis of polyaniline nanoarrays on graphene oxide for high-performance supercapacitors. Electrochim Acta 265:379–390. https://doi.org/10.1016/j.electacta.2018.01.166
69. Tan YB, Lee J-M (2013) Graphene for supercapacitor applications. J Mater Chem A 1(47):14814–14843. https://doi.org/10.1039/C3TA12193C
70. Usman M, Pan L, Asif M, Mahmood Z (2015) Nickel foam–graphene/MnO_2/PANI nanocomposite based electrode material for efficient supercapacitors. J Mater Res 30(21):3192–3200. https://doi.org/10.1557/jmr.2015.271
71. Wang J-G, Yang Y, Huang Z-H, Kang F (2013a) A high-performance asymmetric supercapacitor based on carbon and carbon–MnO_2 nanofiber electrodes. Carbon 61:190–199. https://doi.org/10.1016/j.carbon.2013.04.084
72. Wang K, Huang J, Wei Z (2010) Conducting polyaniline nanowire arrays for high performance supercapacitors. J Phys Chem C 114(17):8062–8067. https://doi.org/10.1021/jp9113255
73. Wang L, Ye Y, Lu X, Wen Z, Li Z, Hou H, Song Y (2013b) Hierarchical nanocomposites of polyaniline nanowire arrays on reduced graphene oxide sheets for supercapacitors. Sci Rep 3:3568. https://doi.org/10.1038/srep03568
74. Wang X, Deng J, Duan X, Liu D, Guo J, Liu P (2014) Crosslinked polyaniline nanorods with improved electrochemical performance as electrode material for supercapacitors. J Mater Chem A 2(31):12323–12329. https://doi.org/10.1039/C4TA02231A
75. Wang X, Wu D, Song X, Du W, Zhao X, Zhang D (2019) Review on carbon/polyaniline hybrids: design and synthesis for supercapacitor. Molecules 24(12). https://doi.org/10.3390/molecules24122263
76. Wang Z, Qe Z, Long S, Luo Y, Yu P, Tan Z, Bai J, Qu B, Yang Y, Shi J, Zhou H, Xiao Z-Y, Hong W, Bai H (2018) Three-dimensional printing of polyaniline/reduced graphene oxide composite for high-performance planar supercapacitor. ACS Appl Mater Interfaces 10(12):10437–10444. https://doi.org/10.1021/acsami.7b19635
77. Wei W, Cui X, Chen W, Ivey DG (2011) Manganese oxide-based materials as electrochemical supercapacitor electrodes. Chem Soc Rev 40(3):1697–1721. https://doi.org/10.1039/C0CS00127A
78. Wu X, Wu G, Tan P, Cheng H, Hong R, Wang F, Chen S (2018) Construction of microfluidic-oriented polyaniline nanorod arrays/graphene composite fibers for application in wearable micro-supercapacitors. J Mater Chem A 6(19):8940–8946. https://doi.org/10.1039/C7TA11135E
79. Wu Z-S, Ren W, Wang D-W, Li F, Liu B, Cheng H-M (2010) High-energy MnO_2 nanowire/graphene and graphene asymmetric electrochemical capacitors. ACS Nano 4(10):5835–5842. https://doi.org/10.1021/nn101754k
80. Xia C, Xie Y, Wang W, Du H (2014) Fabrication and electrochemical capacitance of polyaniline/titanium nitride core–shell nanowire arrays. Synth Met 192:93–100. https://doi.org/10.1016/j.synthmet.2014.03.018
81. Yan Y, Cheng Q, Wang G, Li C (2011) Growth of polyaniline nanowhiskers on mesoporous carbon for supercapacitor application. J Power Sources 196(18):7835–7840. https://doi.org/10.1016/j.jpowsour.2011.03.088
82. Yan Y, Li B, Guo W, Pang H, Xue H (2016) Vanadium based materials as electrode materials for high performance supercapacitors. J Power Sources 329:148–169. https://doi.org/10.1016/j.jpowsour.2016.08.039
83. Yang G, Takei T, Yanagida S, Kumada N (2019) Hexagonal tungsten oxide-polyaniline hybrid electrodes for high-performance energy storage. Appl Surf Sci 498:143872. https://doi.org/10.1016/j.apsusc.2019.143872
84. Yanilmaz M, Dirican M, Asiri AM, Zhang X (2019) Flexible polyaniline-carbon nanofiber supercapacitor electrodes. J Energy Storage 24:100766. https://doi.org/10.1016/j.est.2019.100766

85. Ye Y-J, Huang Z-H, Song Y, Geng J-W, Xu X-X, Liu X-X (2017) Electrochemical growth of polyaniline nanowire arrays on graphene sheets in partially exfoliated graphite foil for high-performance supercapacitive materials. Electrochim Acta 240:72–79. https://doi.org/10.1016/j.electacta.2017.04.025
86. Yu A, Chabot V, Zhang J (2013a) Electrochemical supercapacitors for energy storage and delivery: fundamentals and applications. CRC Press
87. Yu L, Zhang G, Yuan C, Lou XW (2013b) Hierarchical $NiCo_2O_4$@MnO_2 core–shell heterostructured nanowire arrays on Ni foam as high-performance supercapacitor electrodes. Chem Commun 49(2):137–139. https://doi.org/10.1039/C2CC37117K
88. Yu P, Zhang Z, Zheng L, Teng F, Hu L, Fang X (2016) A novel sustainable flour derived hierarchical nitrogen-doped porous carbon/polyaniline electrode for advanced asymmetric supercapacitors. Adv Energy Mater 6(20):1601111. https://doi.org/10.1002/aenm.201601111
89. Zhai Y, Dou Y, Zhao D, Fulvio PF, Mayes RT, Dai S (2011) Carbon materials for chemical capacitive energy storage. Adv Mater 23(42):4828–4850. https://doi.org/10.1002/adma.201100984
90. Zhang H, Cao G, Wang Z, Yang Y, Shi Z, Gu Z (2008) Tube-covering-tube nanostructured polyaniline/carbon nanotube array composite electrode with high capacitance and superior rate performance as well as good cycling stability. Electrochem Commun 10(7):1056–1059. https://doi.org/10.1016/j.elecom.2008.05.007
91. Zhang J, Jiang J, Li H, Zhao XS (2011) A high-performance asymmetric supercapacitor fabricated with graphene-based electrodes. Energy Environ Sci 4(10):4009–4015. https://doi.org/10.1039/C1EE01354H
92. Zhang X, Ma L, Gan M, Fu G, Jin M, Zhai Y (2018) Controllable constructing of hollow MoS2/PANI core/shell microsphere for energy storage. Appl Surf Sci 460:48–57. https://doi.org/10.1016/j.apsusc.2017.10.010
93. Zhang Y, Zhang JM, Hua Q, Zhao Y, Yin H, Yuan J, Dai Z, Zheng L, Tang J (2019) Synergistically reinforced capacitive performance from a hierarchically structured composite of polyaniline and cellulose-derived highly porous carbons. Mater Lett 244:62–65. https://doi.org/10.1016/j.matlet.2019.02.045
94. Zhao C, Ang JM, Liu Z, Lu X (2017) Alternately stacked metallic 1T-MoS2/polyaniline heterostructure for high-performance supercapacitors. Chem Eng J 330:462–469. https://doi.org/10.1016/j.cej.2017.07.129
95. Zheng H, Ou JZ, Strano MS, Kaner RB, Mitchell A, Kalantar-zadeh K (2011) Nanostructured tungsten oxide—properties, synthesis, and applications. Adv Func Mater 21(12):2175–2196. https://doi.org/10.1002/adfm.201002477
96. Zheng X, Yu H, Xing R, Ge X, Sun H, Li R, Zhang Q (2018) Multi-growth site graphene/polyaniline composites with highly enhanced specific capacitance and rate capability for supercapacitor application. Electrochim Acta 260:504–513. https://doi.org/10.1016/j.electacta.2017.12.100
97. Zhou Y, Guo W, Li T (2019) A review on transition metal nitrides as electrode materials for supercapacitors. Ceram Int 45(17, Part A):21062–21076. https://doi.org/10.1016/j.ceramint.2019.07.151
98. Zhou Z, Liu K, Lai C, Zhang L, Li J, Hou H, Reneker DH, Fong H (2010) Graphitic carbon nanofibers developed from bundles of aligned electrospun polyacrylonitrile nanofibers containing phosphoric acid. Polymer 51(11):2360–2367. https://doi.org/10.1016/j.polymer.2010.03.044
99. Zou Y, Zhang Z, Zhong W, Yang W (2018) Hydrothermal direct synthesis of polyaniline, graphene/polyaniline and N-doped graphene/polyaniline hydrogels for high performance flexible supercapacitors. J Mater Chem A 6(19):9245–9256. https://doi.org/10.1039/C8TA01366G